Draft version May 13, 2023
Typeset using LaTeX **twocolumn** style in AASTeX631

Polarization of Radiation Emitting From Around Spinning Black Holes

A. Palaoro[1]

[1] *Department of Astronomy, University of Virginia*

ABSTRACT

Black hole simulations have become increasingly relevant and necessary with the imaging from the Event Horizon Telescope of M87 and Sgr A* and polarization images from the Imaging X-ray Polarimetry Explorer. Building off of `Athena++` modifications made by previous students, and the previous `geokerr` and `ipole` codes by Dexter & Agol (2009) and Mościbrodzka & Gammie (2018) respectively, the polarization results were examined closely and found to be erring. A re-implementation of the parallel transportation methods by Dexter (2016) showed the same polarization, meaning the original method wasn't wrong and there was some other error, likely in the initialization and interpretation of the black hole. Intensity was consistently correct across black holes, but the polarization fraction showed behaviour at higher energies that was inconsistent with what Schnittman & Krolik (2009) found, and inconsistent with theory. Polarization angle was less drastic in error, but could still be seen with anomalous behaviours at higher energies. It is likely the problem lies in how the Stokes vectors are being computed as their individual magnitudes aren't consistent with what they should be, and will need to be revisited, along with the initialization of the black hole problem since photon wave vectors mostly matched when implementing different methods. This thesis is submitted in partial completion of the requirements of the BS Astronomy-Physics Major.

Keywords: accretion, accretion discs, black hole physics, radiative transfer, relativistic processes

1. INTRODUCTION

Spin effects are short range, as opposed to effects from mass, and so are more difficult to measure. These two parameters are of particular interest as the physics of stationary black holes are completely specified by the mass and spin in general relativity, assuming negligible electric charge. Observations of X-ray intensity and polarization from the accretion disk of a black hole can be used to verify model accuracy for well constrained black holes, and to further infer the spin from fitting the model to observational data.

Recent images released of the M87 black hole and Sgr A*, as published by The Event Horizon Telescope Collaboration et al. (2019, 2022), allows for the comparison between observational data and radiative models of the general relativistic magnetohydrodynamics (GRMHD) involved with black holes. In addition, the measurements of the polarization done by the Imaging X-Ray Polarimetry Explorer (IXPE) allows the computational models for polarization to be refined to the point of reliably being able to determine the spin of black holes from the measured polarization of radiation from their accretion disks, as per one of the scientific goals of the IXPE mission.

The framework of `Athena++` was used and expanded upon by previous students for the calculation of the radial coordinates of photon impact and the α and β impact parameters, with numerical methods for parallel transporting the polarized radiation based on the `GRTRANS` code by Dexter (2016) and the quasi-analytical methods of the `ipole` code by Mościbrodzka & Gammie (2018). `GRTRANS` uses the Kerr metric to parallel transport a photon's polarization basis along a geodisc to calculate polarization; `ipole` parallel transports a coherency tensor and evolves the Stokes parameters.

Our version of the Athena++ framework uses Monte Carlo simulations to calculate individual photon parameters at discrete points in contrast to the continuous curves currently used in `GRTRANS` and `ipole`. This allows for more flexibility in the choice of photon energies and further implementation for other objects with similar polarizing properties such as X-ray binaries and luminous accretion flows.

While the radiation emitting from the accretion disk thought to be unpolarized, the spacetime near a black hole is curved causing the light to become polarized to

an observer. Accounting for effects like beaming, lensing, and frame-dragging by use of general relativity and the Kerr metric is needed to calculate the polarization accurately.

2. METHODS

Previous results of this code (see: Rohr (2020), Phillips (2021)) were examined and used to create intensity spectra and polarization fraction and angle spectra by integrating over the individual images, each generated for a single energy, to get these spectra as functions of frequency. The spectra were created for a variety of spins and camera inclination angles, as in Figures 7, and 8. Comparison to the spectra of Schnittman & Krolik (2009) shows that our polarization differs from theirs. Since other people have confirmed their results, we came to the conclusion that our polarization was being calculated incorrectly. The intensity spectra was consistent with the verified results.

To look further into this a recreation of Dexter's 2016 methods was created, since his results have been verified, however we continued to use the radius coordinate, and impact parameters α and β from each photon from our modified `Athena++` code since that has been well tested. This allows for a comparison between results and determines more of where our code errs.

The path of emitted photons affected by curved spacetime are assumed to be geodesics in the Kerr metric and are calculated with the geodesic Equations 1.

$$\frac{d\mathbf{x}^\mu}{d\lambda} = \mathbf{k}^\mu \tag{1a}$$

$$\frac{d\mathbf{k}^\mu}{d\lambda} = -\Gamma^\mu_{\alpha\beta}\mathbf{k}^\alpha\mathbf{k}^\beta \tag{1b}$$

$$\Gamma^\alpha_{\beta\gamma} = \frac{1}{2}g^{\alpha\delta}(g_{\delta\beta\gamma} + g_{\delta\gamma\beta} - g_{\beta\gamma\delta}) \tag{1c}$$

Following the execution in Dexter (2016), photons in the comoving frame are transported between a camera at inclination $\mu_0 = \cos\theta_0$ normal to the disk plane at the boundary of the simulation to the point of impact at $\theta = \pi/2$. The dimensionless constants of motion for a given α and β are then given by

$$l = -\alpha\sqrt{1-\mu_0^2} \tag{2a}$$

$$q^2 = \beta^2 + \mu_0^2(\alpha^2 - a^2), \tag{2b}$$

with the additional parameter a that specifies the black hole spin; l is the z-component of the angular momentum, and q^2 is Carter's constant.

The photon wave vector $\mathbf{k}^\mu$, defined by Equations 3, and Walker-Penrose constants, defined by Equation 5, in the Kerr metric partially describe the polarization basis f^μ. Correcting the form of $\mathbf{k}^r$ that appears in Dexter (2016),

$$\mathbf{k}^t = \frac{1}{\rho^2}\left[-a\left(a\sin^2\theta - l\right) + \frac{\left(r^2+a^2\right)}{\Delta}\left(r^2 + a^2 - al\right)\right] \tag{3a}$$

$$\mathbf{k}^r = -\frac{s_r * r * \sqrt{R(r)}}{\rho^2} \tag{3b}$$

$$\mathbf{k}^\theta = -\frac{s_\theta}{\rho^2}\sqrt{\frac{M(\theta)}{\sin^2\theta}} \tag{3c}$$

$$\mathbf{k}^\phi = \frac{1}{\rho^2}\left[-a + \frac{l}{\sin^2\theta} + \frac{a}{\Delta}(r^2 + a^2 - al)\right] \tag{3d}$$

where

$$M(\theta) = q^2 + \left(a^2 - q^2 - l^2\right)\cos^2\theta - a^2\cos^4\theta \tag{4a}$$

$$R(r) = r^2 + (a^2 - q^2 - l^2) + 2\left[(a-l)^2 + q^2\right]r^{-1} - a^2q^2r^{-2} \tag{4b}$$

$$\rho^2 = r^2 + a^2\cos^2\theta \tag{4c}$$

$$\Delta = r^2 - 2r + a^2 \tag{4d}$$

The direction is specified by signs s_r and s_θ, here understood as $s_r = s_\theta = 1$, and

$$K_1 - iK_2 = (r - ia\cos\theta)\left\{(\mathbf{k}^t f^r - \mathbf{k}^r f^t) + a\sin^2\theta(\mathbf{k}^r f^\phi - \mathbf{k}^\phi f^r) - i[(r^2+f^2)(\mathbf{k}^\phi f^\theta - f^\phi\mathbf{k}^\theta) - a(\mathbf{k}^t f^\theta - \mathbf{k}^\theta f^t)]\sin\theta\right\} \tag{5}$$

Two sets of initial K_1 and K_2, found by the asymptotic form of equation 5, were used in order to compute the polarization components in the tetrad frame for the two basis vectors $\hat{\phi}_\mathbf{0}$ and $\hat{\theta}_\mathbf{0}$; they are given by $K_1 = -\gamma$, $K_2 = -\beta$ and $K_1 = -\beta$, $K_2 = \gamma$, where $\gamma = -\alpha - a\sin\theta_0$. The covariant metric components, $g_{\mu\nu}$, are calculated as

$$g_{tt} = -\frac{1}{\rho^2\Delta}\left[\left(r^2+a^2\right)^2 - a^2\Delta\sin^2\theta\right] \tag{6a}$$

$$g_{\phi t} = \frac{-2ar\sin^2\theta}{\rho^2} \tag{6b}$$

$$g_{rr} = \frac{\rho^2}{\Delta} \tag{6c}$$

$$g_{\theta\theta} = \rho^2 \tag{6d}$$

$$g_{\phi\phi} = \frac{\Sigma\sin^2\theta}{\rho^2} \tag{6e}$$

where

$$\Sigma = (r^2+a^2)^2 - a^2\Delta\sin^2\theta \tag{7}$$

The components of f^μ can then be calculated in the tetrad frame using $g_{\mu\nu}$ alongside the polarization basis constants γ and δ.

$$\delta_1 = r\mathbf{k}^t - ra\sin^2\theta\mathbf{k}^\phi \tag{8a}$$
$$\delta_2 = a^2\sin\theta\cos\theta\mathbf{k}^t - a\cos\theta\sin\theta(r^2+a^2)\mathbf{k}^\phi \tag{8b}$$
$$\delta_3 = ra\sin^2\theta\mathbf{k}^r + a\cos\theta\sin\theta(r^2+a^2)\mathbf{k}^\theta \tag{8c}$$
$$\gamma_1 = a\cos\theta\mathbf{k}^t - a^2\cos\theta\sin^2\theta\mathbf{k}^\phi \tag{8d}$$
$$\gamma_2 = r(r^2+a^2)\sin\theta\mathbf{k}^\phi - ar\sin\theta\mathbf{k}^t \tag{8e}$$
$$\gamma_3 = a^2\cos\theta\sin^2\theta\mathbf{k}^r - r(r^2+a^2)\sin\theta\mathbf{k}^\theta. \tag{8f}$$

$$f^r = \frac{1}{N}\left[(\gamma_2K_1 - \delta_2K_2)(g_{\phi\phi}\mathbf{k}^\phi + g_{\phi t}\mathbf{k}^t) - (\gamma_3K_1 - \delta_3K_2)g_{\theta\theta}\mathbf{k}^\theta\right] \tag{9a}$$
$$f^\theta = -\frac{1}{N}\left[(\gamma_1K_1 - \delta_1K_2)(g_{\phi\phi}\mathbf{k}^\phi + g_{\phi t}\mathbf{k}^t) - (\gamma_3K_1 - \delta_3K_2)g_{rr}\mathbf{k}^r\right] \tag{9b}$$
$$f^\phi = \frac{1}{N}\left[(\gamma_1K_1 - \delta_1K_2)g_{\theta\theta}\mathbf{k}^\theta - (\gamma_2K_1 - \delta_2K_2)g_{rr}\mathbf{k}^r\right] \tag{9c}$$
$$N = (\gamma_2\delta_1 - \gamma_1\delta_2)g_{\phi\phi}\mathbf{k}^\phi - (\gamma_3\delta_1 - \gamma_1\delta_3)g_{\theta\theta}\mathbf{k}^\theta + (\gamma_2\delta_1 - \gamma_1\delta_2)g_{\phi t}\mathbf{k}^t + (\gamma_3\delta_2 - \gamma_2\delta_3)g_{rr}\mathbf{k}^r \tag{9d}$$

Equation 9d is a corrected form of that found in Dexter (2016). Differentiating which pair of the Walker-Penrose tensor constant components was used for the two polarization basis vectors in f^μ by a subscript, the stokes parameters can be calculated in the coordinate frame as the rotation elements

$$\sin 2\chi = -2\frac{\left(f_0^\theta \cdot f_1^\theta\right)}{\left(f_0^\theta\right)^2 + \left(f_1^\theta\right)^2} \tag{10a}$$
$$\cos 2\chi = \frac{\left(f_1^\theta\right)^2 - \left(f_0^\theta\right)^2}{\left(f_0^\theta\right)^2 + \left(f_1^\theta\right)^2} \tag{10b}$$

The major comparisons were made between the two methods for calculating the photon wave vector $\mathbf{k}^\mu$, since both the rotation elements and that which composes them are functions of $\mathbf{k}^\mu$.

3. RESULTS

Photon lists were simulated for a variety of spins, 0 and 0.9, and camera inclination angles, 45°, 60° and 75°. This allowed for the comparison of results to multiple other people's results even if their initial parameters are ambiguous. It also, incorrectly, shows the effect of spin and inclination on the observed radiation of accretion disks.

3.1. *Tests*

Tests comparing the wave vectors from the Monte Carlo and Dexter (2016) methods show that they agree to 0.1%, except for $\mathbf{k}^\phi$ which has a ±7% disagreement. While not ideal, even the 7% is unlikely to produce spectra with behaviour completely different from other models.

3.2. *Images with Polarization Direction*

The selection of images generated show intensity that is consistent throughout various literature (Dexter (2016), Schnittman & Krolik (2009)), with a representative example being the intensity plot in Figure 1. What is deviant from prior results are the polarization vectors, especially as they near the center of the black hole.

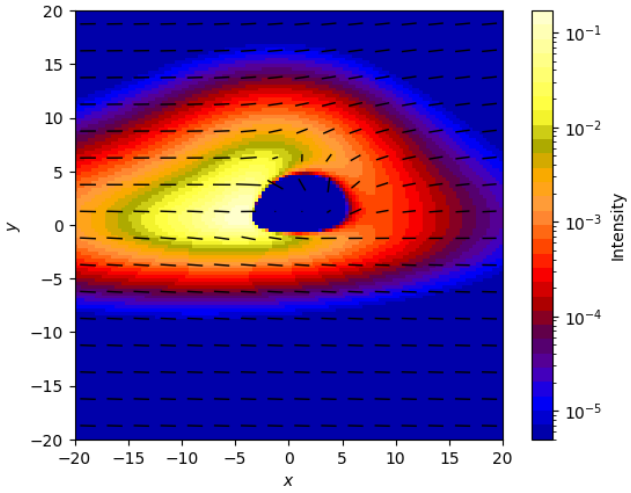

Figure 1: Intensity and linear polarisation map of thermal emission from a thin accretion disc, including only the effects of direct radiation. The black hole has spin 0.9 and an inclination angle of 75°. The image is log-scaled with a color scale to resemble previous results of Schnittman & Krolik (2009) and Dexter (2016).

As an individual simulation, the polarization doesn't look so wrong as to be obvious, except that the polarization fraction, visualized as the length of the vectors, nearest to the innermost stable circular orbit (ISCO) is larger than expected. Similar results can be seen for other spins and inclinations. Higher spin exacerbates the errors, which are only present closer to the ISCO where higher energy radiation is emitted.

Spin 0 still has incorrect polarization vectors though, as in Figure 6a, as the polarization fraction is expected to decrease since each vector is meant to be representative of the average in that cell. Figures 6 show the

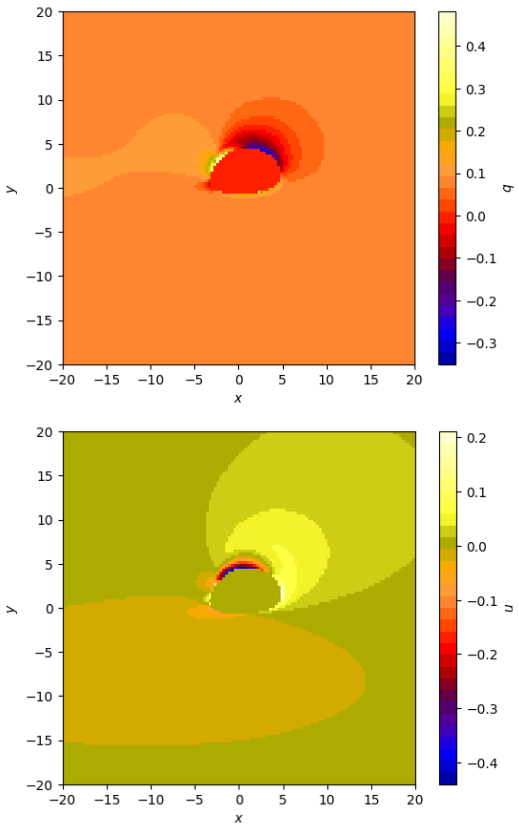

Figure 2: Plots of the intensity-normalized Stokes parameters q (left) and u (right) for spin 0.9 and camera angle 75°.

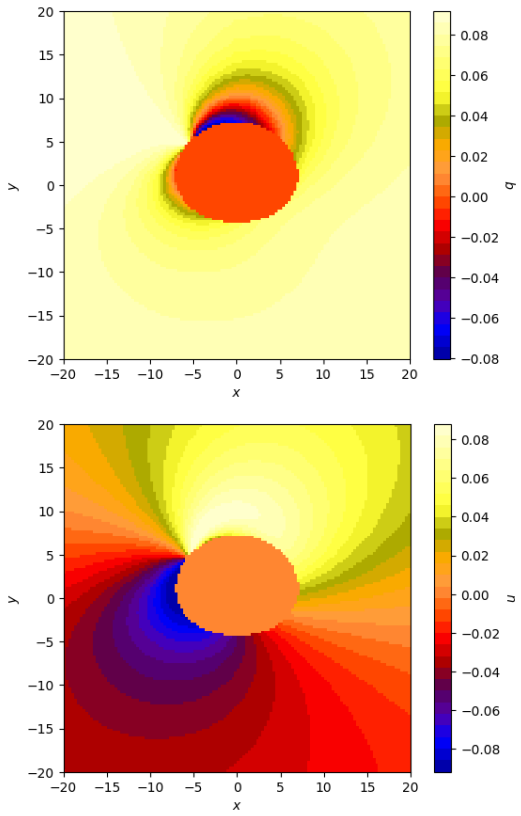

Figure 3: Plots of the intensity-normalized Stokes parameters q (left) and u (right) for spin 0 and camera angle 45°.

changes as spin and inclination change. While the polarization angles decrease nearer the ISCO, excluding spin 0.9 and angle 75°, they do so far more than expected. What is very unexpected is that the polarization vector gets longer closer to the ISCO, which while is reasonable for individual photons, since the images are made of small averages, the orientation of the vectors should mean that the magnitude of the polarization vector is overall smaller. Images of the relevant Stokes parameters were also generated in a similar manner so as to better determine what is incorrect.

Figure 3 shows the Stokes parameters for an equivalent black hole to Figure 1 and are behaviourally equivalent to the rotation elements of Dexter (2016). They are expected to fall between 0 and 1, and sum to 1, but they fall short; the behaviour across locations does roughly resemble the expected results if discounting the overall magnitude. Further images of the intensity and individual Stokes parameters for different initial conditions are near the end for comprehensiveness, though all show similar behaviours.

3.3. *Spectra with Polarization Angle and Fraction*

As mentioned, the spectra of intensity and polarization angle and fraction were computed, giving them as functions of frequency and shows the overall behaviour of the polarization. The comparative graphs were made in the fashion of Schnittman & Krolik (2009).

Figure 5 shows the convergence for different photon resolutions for both spin 0 and spin 0.9, but the same camera angle, demonstrating that any errors aren't on account of too low of a photon resolution causing incorrect cell averaging. This is consistent with spin 0 and other inclinations as well.

Relativistic effects are strongest nearest to the black hole, ergo the measured polarization fraction from each photon is largest there too. When *averaging over an area* near the center then, the polarization angle and degree appear to be *lower* because of the diverging directions within a single mesh cell. The Stokes parameters can be seen as not having a large enough magnitude to correctly cancel each other out, which is only noticeable nearest to the black hole because of how small the polarization is far away.

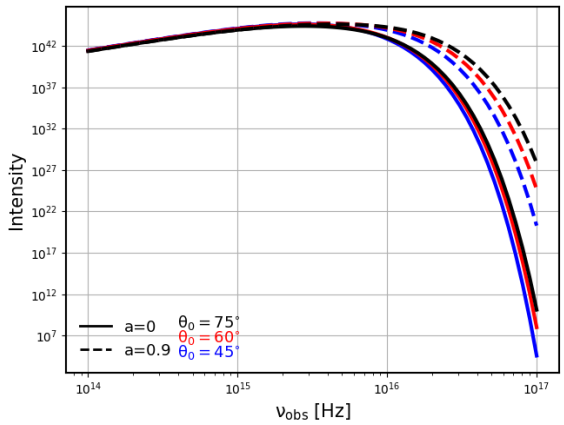

Figure 4: Intensity spectra from direct radiation of photons in the 1e14 to 1e17 Hz band from the accretion disk of black holes with various spins and inclinations. The behaviour is as expected and resembles a blackbody.

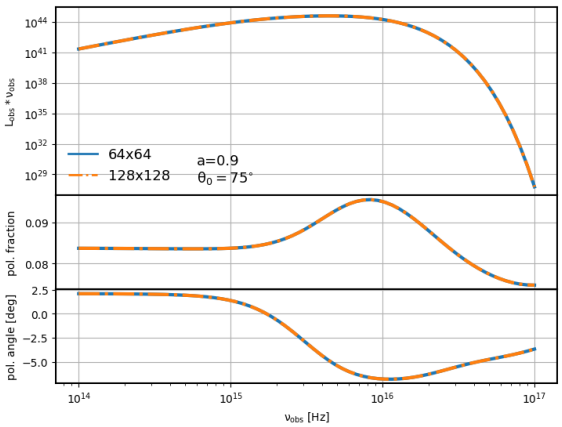

Figure 5: Spectra of intensity and polarization of a spin 0.9 black hole with inclination angle 75°. The curves differ only in photon resolution, with photon counts of 4,096 (blue solid) and 16,384 (orange dashed).

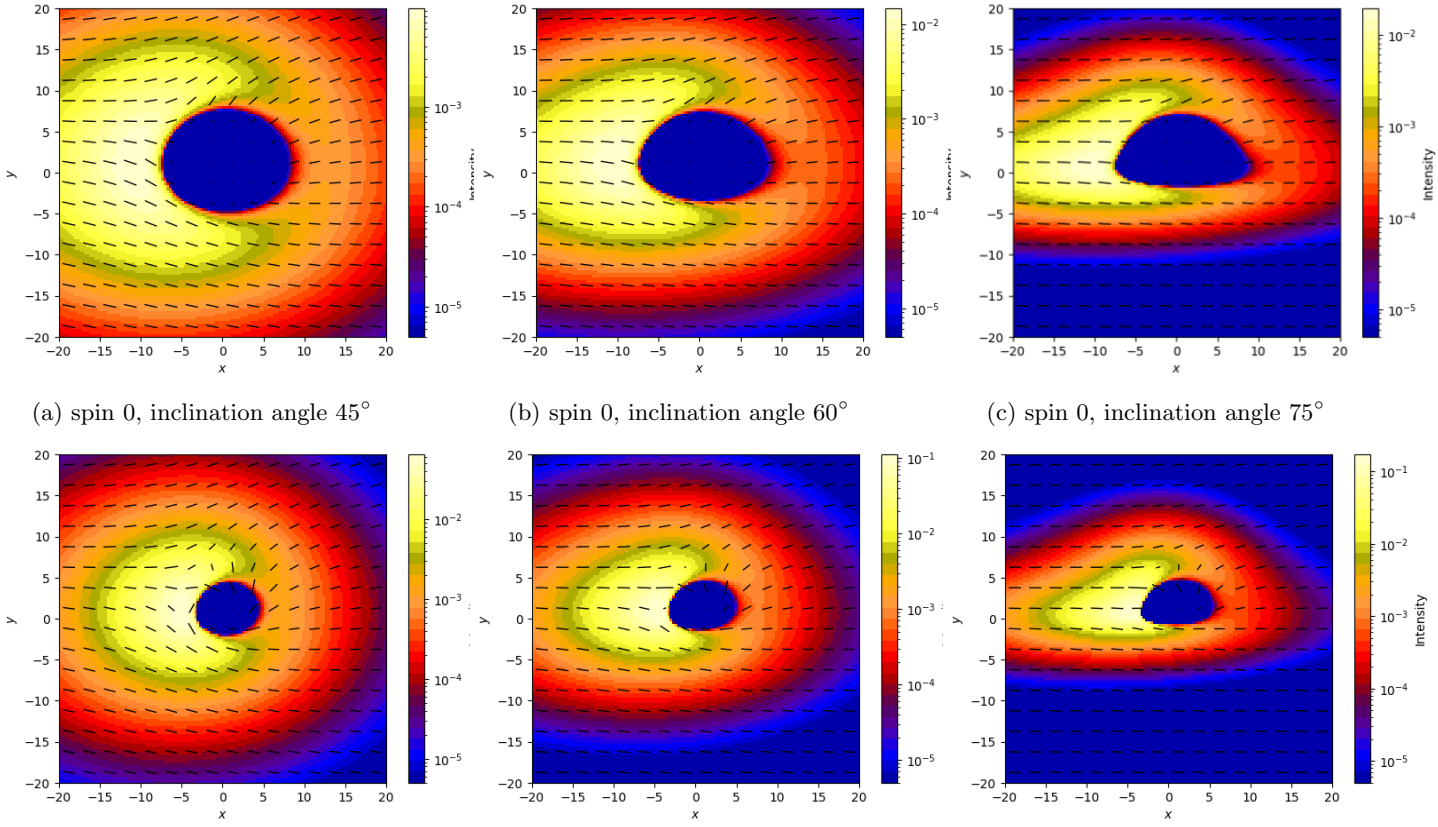

(a) spin 0, inclination angle 45°

(b) spin 0, inclination angle 60°

(c) spin 0, inclination angle 75°

(d) spin 0.9, inclination angle 45°

(e) spin 0.9, inclination angle 60°

(f) spin 0.9, inclination angle 75°

Figure 6: Plots of intensity with polarization overlaid for thin disk black hole models including only the effects of direct radiation. The colormap is logarithmic and chosen to be similar to previous results of Schnittman & Krolik (2009) and Dexter (2016), and the polarization is sampled at a rate of one for every eight intensity pixels. These are all simulated with a black hole with mass $M = M_{bh}$, with the only variables being the inclination angle and spin.

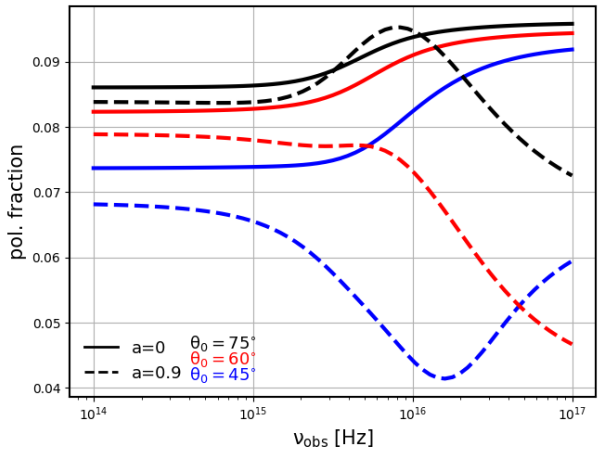

Figure 7: Polarization fraction from direct radiation of photons in the 1e14 to 1e17 Hz band from the accretion disk of black holes with various spins and inclinations. Spinning black holes are dashed curves throughout all figures, and non-spinning black holes are solid curves.

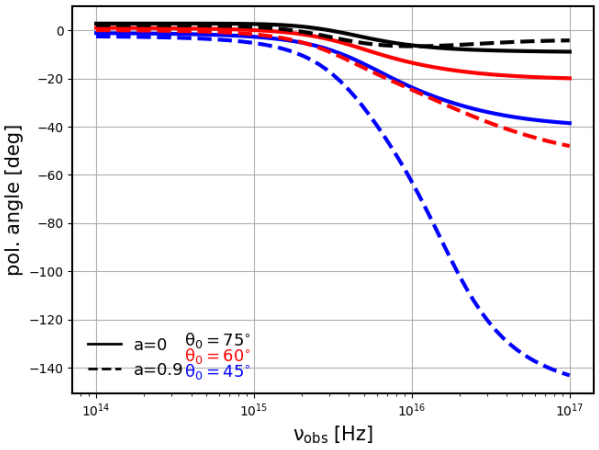

Figure 8: Polarization angle from direct radiation of photons in the 1e14 to 1e17 Hz band from the accretion disk of black holes with various spins and inclinations.

4. DISCUSSION AND CONCLUSION

Evidently the polarization does not average correctly, and doesn't decrease at higher energies near the black hole, likely because the magnitudes of the Stokes parameters that make up the polarization fraction and angle aren't the correct magnitude. While the polarization is incorrect, the intensity is correct and integration shows a blackbody curve. The consistency between the two models suggests that the error was implemented into both and we are doing something wrong in that implementation, and that both how we set up the problem and where ambiguity might lie in other's description of their initialization.

The Monte Carlo method still allows for a highly efficient way to numerically simulate radiation from black holes, and while as of now the polarization only accounts for direct emission, it can be expanded to include reflected radiation, which has a noticeable effect on the polarization of the black hole. It also allows for the usage of the code to simulate similar astrophysical objects that emit polarized X-rays. Having a variety of working models will be increasingly important to compare results and interpretation of observations resulting from both the EHT and IXPE missions.

REFERENCES

Dexter, J. 2016, Monthly Notices of the Royal Astronomical Society, 462, 115–136, doi: 10.1093/mnras/stw1526

Dexter, J., & Agol, E. 2009, The Astrophysical Journal, 696, 1616, doi: 10.1088/0004-637X/696/2/1616

Mościbrodzka, M., & Gammie, C. F. 2018, Monthly Notices of the Royal Astronomical Society, 475, 43–54, doi: 10.1093/mnras/stx3162

Phillips, C. 2021, doi: 10.18130/Z1SR-P854

Rohr, E. 2020, doi: 10.18130/V3-0EN5-AV02

Schnittman, J. D., & Krolik, J. H. 2009, The Astrophysical Journal, 701, 1175–1187, doi: 10.1088/0004-637X/701/2/1175

The Event Horizon Telescope Collaboration et al. 2019, The Astrophysical Journal Letters, 875, L1, doi: 10.3847/2041-8213/ab0ec7

—. 2022, The Astrophysical Journal Letters, 930, L12, doi: 10.3847/2041-8213/ac6674